7764 *Biochemistry* **2010,** *49,* 7764–7773
DOI: 10.1021/bi100880d

BIOCHEMISTRY
including biophysical chemistry & molecular biology
Article

Off-Pathway Status for the Alkali Molten Globule of Horse Ferricytochrome *c*[†]

Abani K. Bhuyan*

School of Chemistry, University of Hyderabad, Hyderabad 500046, India

Received May 31, 2010; Revised Manuscript Received August 4, 2010

ABSTRACT: The Na^+-stabilized alkali molten globule (B-state) of horse ferricytochrome *c* produced at pH 12.9 in 2 M NaCl has been studied to find out its relevance to the kinetic folding pathway of the protein. Details of stopped-flow kinetics indicate that the B-state when driven to fold at pH 11.5 goes through a submillisecond burst expansion to a state B′ which must unfold to the base-denatured U_B-state before folding to the alkaline native state, N_B. This folding hallmark suggests that the B-state is a dead-end or off-pathway species, playing apparently an unclear role in the folding kinetics. Interestingly, the folding kinetics of the B-state at a final pH of 7 is very similar to that observed for the guanidinium-unfolded ferricytochrome *c* (U) at pH 7. Both B and U exhibit a submillisecond burst phase followed by three observable phases, fast, medium, and slow, with matching rate constants for the fast phase, suggesting that B- and U-states share a common folding mechanism. Even the minima in the folding chevrons for the B- and U-states appear at the same denaturant concentration, but the former is shifted vertically upward and has shallower limbs, suggesting that the transition state relevant for the B-state folding is relatively more compact with greater surface burial allaying large-scale diffusive migration of chain segments. It is concluded that the B-state is not a good model for the kinetic molten globule of cytochrome *c*. Part of the reason for such atypical response of a typical molten globule may possibly be related to misligation of the ferric heme with lysyl side chains at the extreme alkaline pH required to produce the B-state. To eliminate this possibility, the companion paper [Bhuyan, A. K. (2010) *Biochemistry* (DOI 10.1021/bi100881n)] studies the B-state of ferrocytochrome *c* where ligation of the heme with any intrapolypeptide side chain is completely suppressed. The study concludes that the B-state is kinetically an abortive species.

The concept of the molten globule (MG),[1] "an essentially compact and mobile protein state containing native-like secondary structure and hydrodynamic radius (R_H) but without rigid tertiary structure", has vastly influenced the understanding of protein structure, folding, and function. Intrinsically disordered protein states that lack tertiary structure but are molten globule-like (*1*−*5*) have been found at work in cell signaling and regulatory functions through their interactions with DNA and other proteins (*6*−*12*). The idea that the abundance of molten globule-like proteins increases with evolution and complexity of organisms (*13*) suggests that they are indispensable for cellular function and adaptation.

In the protein folding area, the MG state is often conservatively thought of as a thermodynamic state distinct from the native (N) and unfolded (U) states, implicating its connection with the N ⇌ U phase transition (*14*−*17*). A proof of universal occurrence of MG states in the folding pathway will necessarily imply that protein folding is hierarchic (*14*, *18*−*20*). Considerable evidence for their presence in the folding pathway has come from steady-state and temporal resolution of MG intermediates in the folding−unfolding reaction for a large set of proteins (*21*−*24*). Occurrence of MG-like intermediates very late in the folding run has been detected also in theoretical and computer simulation studies of protein folding (*25*). It is now believed that they largely correspond to late folding intermediates beyond the rate-limiting transition state barrier for folding (*15*, *16*, *26*−*29*), although MG intermediates have also been temporally detected in the early stages of folding of several other proteins (*30*−*36*). A basic rationale of these studies is the notion that equilibrium MG states stabilized at extremes of pH in the presence of salt are reliable models of kinetic folding intermediates (*16*, *35*, *37*). The expectation holds for some proteins where structural correspondence between the equilibrium molten globules and kinetic intermediates has been established (*23*, *30*−*33*, *38*−*40*). More recent evidence indicates that the kinetic and equilibrium molten globule intermediates could also significantly differ in structure (*41*, *42*), suggesting that the assumption of structural correspondence needs to be carefully considered and tested on a larger set of proteins. Such investigations not only extend the understanding of the myriad of folding issues but also are related to elucidation of the physical interactions necessary for acquisition of tertiary fold (*39*).

The study presented in this and the accompanying paper (*43*) examines how the cation-stabilized alkali molten globule of horse cytochrome *c* is placed in the kinetic pathway. Cytochrome *c* in the presence of salt can be transformed into the molten globule state at both extremes of pH. Since the pioneering work of Ohgushi and Wada (*44*), the acid molten globule (A-state) has

[†]Funds for this research were provided by Grants BRB/15/227/2001 and BRB/10/622/2008 from the Department of Biotechnology, Government of India.

*To whom correspondence should be addressed. E-mail: akbsc@uohyd.ernet.in. Phone: 91-40-2313-4810. Fax: 91-40-2301-2460.

[1]Abbreviations: GdnHCl, guanidine hydrochloride; cyt *c*, cytochrome *c*; ferricyt *c*, ferricytochrome *c*; ferrocyt *c*, ferrocytochrome *c*; MG, molten globule; $\Delta G_D°$, Gibbs energy of denaturation in the absence of denaturant; m_g, protein surface area associated with denaturant unfolding transition; A- and B-states, acid and alkali molten globule states, respectively; N, native state at pH 7; N_B, N-state at alkaline pH; U, unfolded state at pH 7; U_B, alkali-denatured state with or without GdnHCl; PFG NMR, pulsed-field-gradient NMR.

 Published on Web 08/05/2010

been studied extensively (*4*, *45*−*55*) and assumed to be a good model for a late intermediate in the kinetic folding pathway (*4*, *28*). Recent work has shown that even alkali-denatured cytochrome *c*, regardless of the oxidation state of the protein, transforms into an archetypal molten globule in the presence of Na^+ (*56*, *57*) which undergoes cold denaturation (*57*). The description of the alkali molten globule (B-state) is scarce, since it has been found for only a few other proteins, including β-lactamase (*58*) and barstar (*59*). The relevance of the equilibrium B-state in the folding kinetics of cytochrome *c*, especially its structural similarity with any kinetic intermediate, is unknown. It is shown here that the B-state despite being a highly qualified MG must initially expand to some extent in order to fold to the native state. The conclusion is reinforced by the accompanying paper (*43*) where the molten globule of ferrocytochrome *c* has been put to test.

MATERIALS AND METHODS

Horse cytochrome *c* (type VI) obtained from Sigma was used without further purification. Buffer components and other chemicals were also from Sigma, ultrapure GdnHCl was from USB Corporation (Cleveland, OH), and D_2O was from Aldrich.

Alkali Denaturation of Ferricyt c. The procedure for this experiment has already been described (*57*). Briefly, 10 μM protein (type VI horse cytochrome *c* purchased from Sigma) prepared in a Tris−Na_2HPO_4−CAPS [3-(cyclohexylamino)-1-propanesulfonic acid] buffer (10 mM each) is held at different pH values in the range 7.5−13.2. Following incubation at 22 °C for ∼30 min, fluorescence of the protein was measured by 280 nm excitation in a FluoroMax-4P instrument (Jobin-Yvon, Horiba). The reported values of pH are the ones measured after fluorescence measurement.

NaCl Titration and GdnHCl Unfolding of Alkali-Denatured Ferricyt c. For experiments under alkaline conditions, two 10 μM stock cytochrome *c* solutions (one without any additive and the other containing 2.5 M NaCl or 3.9 M GdnHCl) prepared in water at pH 13 were appropriately mixed to obtain samples containing a variable amount of NaCl or GdnHCl. Fluorescence spectra were taken at the end of 1 h of incubation. The GdnHCl titration at pH 7 employed a 0.1 M sodium phosphate buffer.

Stopped-Flow Kinetics. Since several sets of refolding experiments were carried out, the initial cyt *c* solution (∼125 μM) was prepared as required by the objective: in 4.2 M GdnHCl, 0.1 M phosphate, pH 7, in 3.75 M GdnHCl, pH 12.9 (±0.1), in 2 M NaCl, pH 12.9 (±0.1), and in aqueous solution at pH 12.9 (±0.1) without an additive. After 0.5 h incubation, refolding was allowed by diluting the unfolded protein solution into 7 volumes of the appropriate refolding buffer of variable GdnHCl content held at pH 7 (0.1 M phosphate), 10.5 (20 mM CAPS), or 12.9 (water) as detailed under the Results section. The refolding buffer contained 2 M NaCl when refolding to the molten globule state was desired. The details of the refolding buffer are also indicated in the text and/or figure legend. The dilution mixings were simulated in a test tube to check if the required pH values are obtained in the mixed solutions. To study unfolding kinetics at pH 7, the native protein solution (∼125 μM) prepared in 0.1 M phosphate was diluted 8-fold into the same buffer containing unfolding concentrations of GdnHCl. After recording kinetics the waste solutions were collected to check the pH value and the GdnHCl content. Fluorescence-probed kinetics were measured at 22 °C using a SFM-400 mixing module (Biologic) equipped with a 0.8 mm cuvette (FC 08). Excitation wavelength was 280 nm, and emission was measured using a 335 nm cutoff filter. Typically, 10−20 shots were averaged. The window in the stopped-flow observation head meant for the fiber optic cable carrying the fluorescence excitation beam was notched toward the mixer side so as to illuminate only the lower half of the cuvette. In this configuration, the measured dead time was 1.3 (±0.2) ms.

NMR Spectroscopy. The samples were D_2O solutions of 2 mM cyt *c* containing variable amount of NaCl held at pH 13.2 unbuffered or at pH 7 in 0.1 M phosphate. Phase-sensitive NOESY spectra (τ_m = 150 ms) were recorded with 512 t_1 and 8012 Hz spectral width. Pulsed-field-gradient NMR (PFG NMR) diffusion measurements were done using the Bruker-implemented water−sLED pulse sequence (*60*) with diffusion gradient (*z*-gradient) strength in the range of 3−50 G cm^{-1}. These spectra were of 32K complex data points for a typical spectral width of 8503 Hz. About 1 mM 1,4-dioxane was added to the protein sample as an internal R_H standard. Values of R_H were calculated by

$$I(g) = A\exp(-kg^2)$$
$$R_H^{protein} = R_H^{dioxane}\left(\frac{k_{dioxane}}{k_{protein}}\right) \quad (1)$$

where *I* is the NMR signal intensity, *g* is the gradient strength, and the decay constant, *k*, is proportional to the diffusion coefficient. All NMR spectra were recorded at 23 (±1) °C in a 500 MHz spectrometer (Avance III; Bruker).

RESULTS

Preparation and Stability of the B-State. The Na^+-induced transformation of ferricyt *c* to a mainstream molten globule under extreme alkaline conditions has been demonstrated earlier in detail (*57*). For a brief orientation here, results of some basic experiments repeated are produced in Figure 1. The fluorescence-probed sharp transition in the 12−12.6 region of pH (Figure 1a) indicates that the tertiary structure unfolds cooperatively to a state called U_B. The N → U_B transition removes nearly all of the tertiary structure, because the unfolded state fluorescence is fully recovered at pH >12.7. The pH midpoint of the titration (C_m = 12.3) and the number of OH^- titrated (n = 3.1) are extracted from

$$y = \frac{s_u + s_f\{10^{n(pH - C_m)}\}}{1 + 10^{n(pH - C_m)}} \quad (2)$$

where s_u and s_f are normalized fluorescence signals for the alkali-denatured and native proteins, respectively. Even though stripped of tertiary fold, the U_B-state contains considerable secondary structure (*57*) that unfolds when GdnHCl is included at pH >12.7.

Figure 1b shows the NaCl-induced U_B → B transition at pH 12.9. The transition, presumably driven by the charge-screening action of Na^+, appears to cause substantial compaction of the molecule because the fluorescence in the presence of 2 M NaCl is as quenched as in the native state. But the mean effective hydrodynamic radii (R_H) for different species measured by pulsed-field-gradient NMR experiments suggest that the average molecular diameter of the B-state is just about 2 Å less than that for the U_B-state (Table 1), implying closeness of the two states in terms of molecular dimension. Also, little tertiary structural constraints are gained in the U_B → B transition as evidenced by the motionally averaged broad resonances in the aliphatic−aromatic

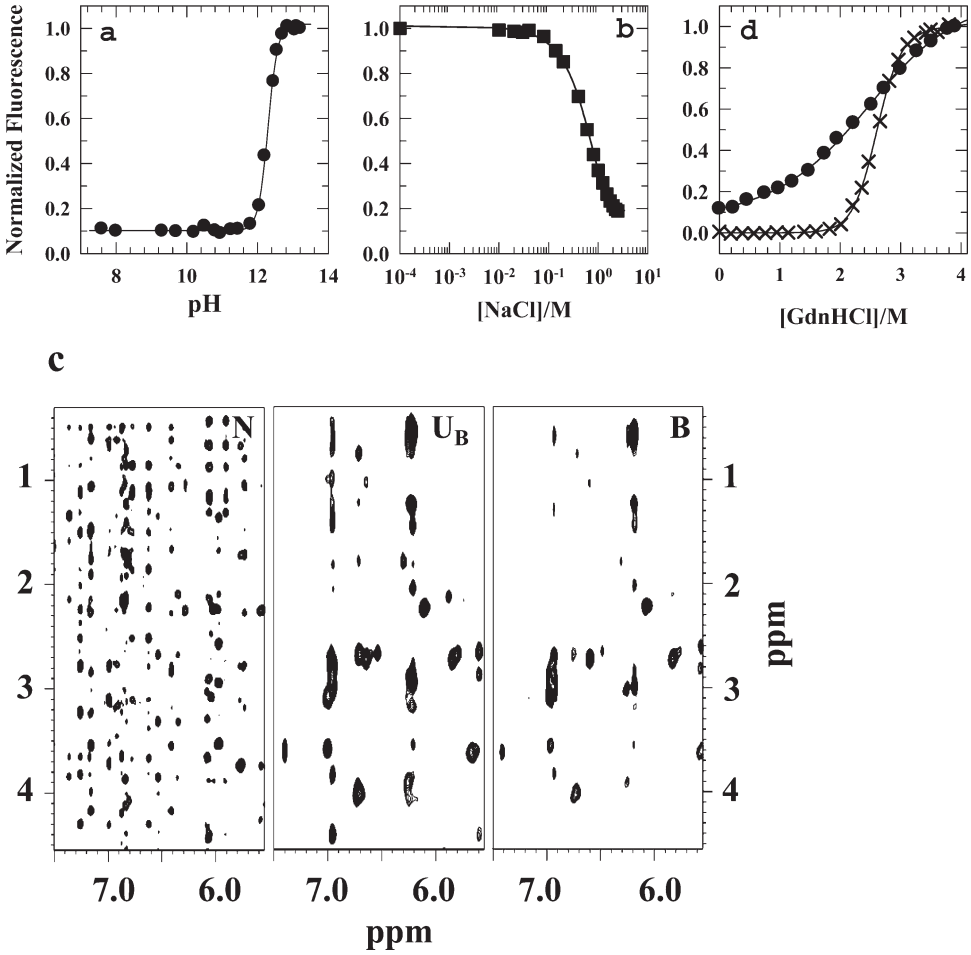

FIGURE 1: Preparation and stability of the B-state. (a) Alkali titration of ferricyt *c* denatures the protein into the U_B-state at pH ~12.8. The fit through the data according to eq 1 provides the pH midpoint of the titration (C_m = 12.3) and the number of OH^- titrated (n = 3.1). (b) The NaCl-induced promotion of U_B to the B-state ($U_B \rightleftharpoons B$) presumably due to charge screening action of Na^+. The $U_B \rightarrow B$ transition is characterized by a large decrease of fluorescence, indicating a compact molecular organization of the B-state. (c) Sections of phase-sensitive NOESY spectra (500 MHz) showing motionally averaged broad resonances for U_B- and B-states. The spectrum for the native state protein at pH 7, 0.1 M phosphate, is also shown as a control. (d) Equilibrium unfolding transitions for the B-state in 2 M NaCl, pH 13 (×), and the native state in 0.1 M phosphate, pH 7 (●). Solid lines through data represent two-state fits ($U_B \rightleftharpoons B$ and $U \rightleftharpoons N$), and the values of $\Delta G°$ and m_g are listed in Table 2. All data were taken at 22 (±1) °C.

Table 1: NMR-Measured Hydrodynamic Radii (R_H) of the Relevant Equilibrium States of Ferricyt *c* at 22 (±1) °C

state	condition	R_H (Å)
N (native)	0.1 M phosphate, pH 7	17.9 (±1.5)
U_B (alkali denatured)	water−NaOH, pH 13.2	23.3 (±1.0)
B (alkali molten globule)	water−NaOH, 2 M NaCl, pH 13.1	22.1 (±0.8)
U (urea unfolded)	0.1 M phosphate, 9 M urea, pH 7	27.9 (±2.3)

side-chain region of the NOESY spectra of U_B- and B-states (Figure 1c), indicating lack of tertiary interactions. To assess the relative stability, Figure 1d compares the GdnHCl unfolding transitions for the B-state (2 M NaCl, pH 13) and the native state of ferricyt *c* (0.1 M phosphate, pH 7). Because there is no evidence for the involvement of equilibrium intermediate for both structural transitions, data were fit to the two-state equilibrium model. Values of $\Delta G°$ for N- and B-states are 7.4 (±0.3) and 2 (±0.4) kcal mol^{-1}, respectively, indicating modest stability of the latter. The m_g values of 2.9 (±0.1) and 0.8 (±0.25) kcal mol^{-1} M^{-1} for the $N \rightleftharpoons U$ and $B \rightleftharpoons U_B$ transitions, respectively, together with the observation of exchange-broadened resonances (Figure 1c) suggest that the B-state lacks a significant hydrophobic core and is structurally fluid-like.

Folding Kinetics of the B-State at Alkaline pH. Generally, molten globules are prepared at extremes of pH in the presence of salt, but their refolding kinetics are performed at a neutral pH in the absence of salt. This change in the solvent condition prevents a direct comparison of equilibrium and kinetic intermediates. The rationale for the set of experiments described in this section was to first examine the folding of the alkali molten globule under alkaline condition itself before proceeding to refolding kinetics at pH 7. The B-state prepared in a 2 M NaCl solution at pH 12.9 was allowed to fold at pH 11.5 in the presence of different final concentrations of GdnHCl and constant 1.5 M NaCl. The folding milieu achieved under these conditions of pH and salt does not support B- and U_B-states (Figure 1a). Samples of kinetic traces in Figure 2 show a systematic increase in the zero-time signal with increasing final concentration of GdnHCl, indicating the presence of one or more ultrafast unfolding phases that are lost within the stopped-flow dead time (1.4 ± 0.2 ms). In the observable time bin, the fluorescence changes in two kinetic phases at all concentrations of GdnHCl, although a slow minor phase sharing < 10% of the total observed amplitude appears when the final denaturant concentration falls below 0.4 M. This phase will be considered negligible henceforth. Of the two major phases, the faster one invariably corresponds to a fluorescence

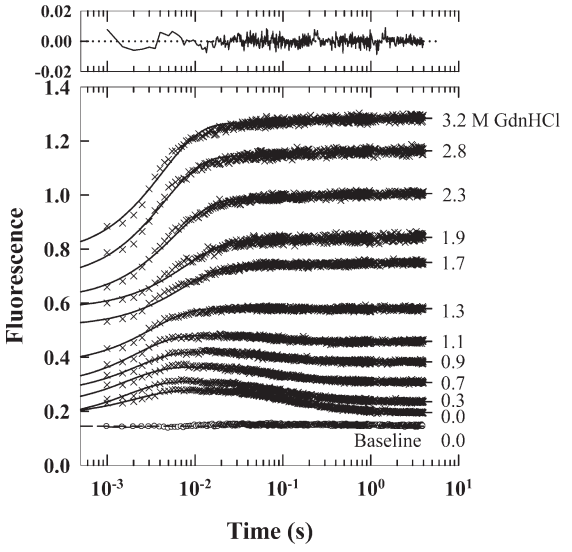

FIGURE 2: Stopped-flow kinetic traces for folding ($B \rightarrow N_B$) and unfolding ($B \rightarrow U$) processes initiated by diluting one part of the B-state solution (2 M NaCl, pH 12.9) into seven parts of 20 mM CAPS buffer, pH 10.5, containing 1.5 M NaCl and variable concentration of GdnHCl. The final pH was 11.5 where the protein folds to N_B or unfolds to U_B depending on the concentration of GdnHCl in the mixed solution. Fit of the data to two or three exponentials shows that all traces register an initial fluorescence increase in two phases, a burst phase and a millisecond phase. The fluorescence then decreases for the traces in the 0−1.3 M range of GdnHCl; the decrease occurs in two phases under strongly refolding condition but is monophasic otherwise. These traces represent the $B \rightarrow N_B$ process. For GdnHCl concentrations higher than ~1.3 M the fluorescence continues to rise mainly by a single phase. These traces represent the $B \rightarrow U_B$ transition.

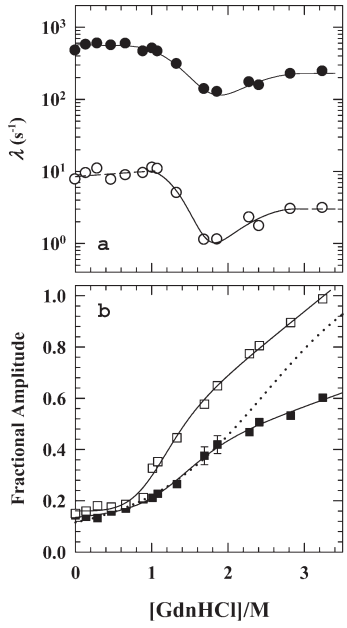

FIGURE 3: GdnHCl distribution of kinetic parameters for folding and unfolding of the B-state at pH 11.5. (a) Chevron plots for the stopped-flow observable initial phase associated with fluorescence increase (●) and the second phase associated with folding and unfolding for the $U_B \rightleftharpoons N_B$ equilibrium (○) as depicted in Scheme 1. The solid lines represent polynomial fits with $m_{f,u}^{\ddagger}/RT$ as coefficients in eq 3. (b) The $t = \infty$ fluorescence (S_∞, □) extracted from fits of the kinetic traces represents the $U_B \rightleftharpoons N_B$ equilibrium transition at pH 11.5. The solid line is a two-state fit (see Table 2). The burst fluorescence signal S_0 (■) obtained by extrapolating the exponential fits to $t = 0$ shows GdnHCl titration of the burst species, B′. The relative shifts of these two transitions suggest that B′ is an unfolding intermediate. The dotted line represents the GdnHCl-induced unfolding of the B-state at pH 12.9 (reproduced from Figure 1d).

rise suggesting an unfolding event (Figure 2). The slower one, associated with a fluorescence decrease at low concentrations of GdnHCl (<1.4 M), is due to protein refolding. At higher denaturant concentration, this slow phase has smaller amplitude and may represent some expansion of the chain (Figure 2). These features alone provide a clue that the burst phase species (B′) enters into a millisecond unfolding process and the product thereof (U_B) folds to N (the fluorescence decaying phase) or slightly expands further (the rising phase) depending on the denaturant-dependent solvent quality in the final medium.

In the absence of GdnHCl in the refolding medium, the apparent rate constants for the fast and slow observable phases (corresponding to the initial unfolding and the final refolding processes, λ_1 and λ_2, respectively) are 472 and 7.6 s^{-1}. Similar difference in the magnitude of λ_1 and λ_2 at all concentrations of GdnHCl produces two discrete chevrons (Figure 3a), the upper one depicting the denaturant dependence of the $B' \rightleftharpoons U_B$. The unfolding of the burst phase product is thus an obligatory event. The appearance of a transition midpoint for each chevron suggests that these millisecond processes are activation barrier-controlled involving changes in structural surfaces, but definite rate rollover under strongly folding and unfolding conditions implies that both processes plausibly involve kinetic intermediates. Since exact modeling of flat arms of folding chevrons is difficult, especially when subsets of experiments are not performed, the available results are qualitatively summarized by the minimal kinetic mechanism shown in Scheme 1. In Scheme 1 I_j and I_k are intermediates invoked based on chevron rollovers (Figure 3a) and N_B is the native state under alkaline condition (pH 11.5). For $j, k > 1$, the intermediates in parentheses possibly equilibrate rapidly in the time scale of folding and unfolding.

Scheme 1

$$B \longrightarrow B' \rightleftharpoons [\cdots I_j \cdots] \rightleftharpoons U_B \rightleftharpoons [\cdots I_k \cdots] \rightleftharpoons N_B$$

The burst formation of B′ is central to the B-state folding under alkaline conditions. For a coarse estimation of its stability and compactness, Figure 3b compares the GdnHCl dependence of the burst fluorescence signal (S_o) relative to the kinetic signal at infinite time (S_∞). The S_∞ curve represents the GdnHCl-induced equilibrium $N_B \rightleftharpoons U_B$ transition at pH 11.5. It is not the $B \rightleftharpoons U_B$ transition, because the B-state is not populated at this pH even in the presence of high salt. A two-state fit of the S_∞ transition yields $\Delta G^\circ \sim 2.4$ kcal mol^{-1}, $m_g \sim 2.3$ kcal mol^{-1} M^{-1}, and $C_m \sim 1.1$ M GdnHCl, indicating that the N-state at this pH (N_B) has roughly the same stability as the B-state (Table 2, rows 1 and 2), notwithstanding the experimental conditions of pH 12.9 for the initial B-state preparation and pH 11.5 for refolding. On the other hand, the GdnHCl titration of the burst phase signal (S_o), which represents the $B \rightarrow B'$ expansion, yields $\Delta G^\circ \sim 2.4$ kcal mol^{-1}, $m_g \sim 1.9$ kcal mol^{-1} M^{-1}, and $C_m \sim 1.3$ M GdnHCl. The two transitions $N_B \rightleftharpoons U_B$ and $B \rightarrow B'$ considered here appear to indicate that B and N_B have nearly similar stability.

To summarize this section, the leading feature of the folding mechanism of the B-state (scheme 1) is the burst formation of a relatively expanded state (B′) which must unfold to U_B before refolding to N_B is feasible. In this sense, the B-state is a dead-end or off-pathway species.

Table 2: Values of $\Delta G°$ (kcal mol^{-1}) and m_g (kcal mol^{-1} M^{-1}) for Fluorescence-Monitored GdnHCl Unfolding of N- and B-States at 22 (±1) °C Extracted from Equilibrium and Kinetic Data

		equilibrium		kinetic	
transition	condition[a]	$\Delta G°$	m_g	$\Delta G°$	m_g
$N_B \rightleftharpoons U_B$	water−NaOH, pH 11.5			2.4 (±0.4)[b]	2.3 (±0.3)[b]
$B \rightleftharpoons U_B$	water−NaOH, pH 13	2.0 (±0.4)	0.8 (±0.2)	2.4 (±0.3)[c]	2.3 (±0.2)[c]
$N \rightleftharpoons U$	0.1 M phosphate, pH 7	7.4 (±1.5)	2.9 (±0.1)	9.1 (±0.6)[d]	3.2 (±0.2)[d]

[a]Refers to final conditions for stopped-flow mixed solutions. The pH and solvent compositions for the preparation of the initial folded (unfolded) protein are given in the text. [b]Values obtained from folding kinetics of the B-state at alkaline pH as discussed under Results (see S_∞ data, □, Figure 3b). [c]From kinetics of the $B \rightleftharpoons U_B$ transition at alkaline pH (see Results and S_∞ data, □, Figure 4c). [d]From folding kinetics carried out under normal conditions (S_∞ data, □, Figure 6a).

Kinetics of the $B \rightleftharpoons U_B$ Transition at Alkaline pH. In this set of experiments, ferricyt *c* initially unfolded in 3.5 M GdnHCl, pH 12.8, and 2 M NaCl was refolded by diluting the denaturant with water under conditions of pH and salt content that matched the initial. Kinetics are described by a missing burst phase and two stopped-flow observable phases (Figure 4a). The rate-denaturant profiles for the two observable phases register a distinct folding chevron for the fast phase only, where the rates roll over at the two chevron extremities and the unfolding rate exceeds the refolding rate by ~8-fold (Figure 4b). The rate constant for the slow phase increases with increments of GdnHCl showing a marginal rate-denaturant gradient and disappears under unfolding conditions (Figure 4b), suggesting that this phase is unlikely to arise from a folding event but perhaps due to unfolding of a small fraction of misfolded/aggregated protein formed after dilution of the denaturant. In the amplitude analyses shown in Figure 4c, the GdnHCl dependence of the t_∞ signal (S_∞) roughly matches the equilibrium $B \rightleftharpoons U_B$ melt (Figure 1c). For a comparison, values of $\Delta G°$ and m_g extracted from the S_∞ GdnHCl data are collated in Table 2. The growing burst signal (S_o) with diminishing GdnHCl concentration (Figure 4c) is indicative of an ultrafast collapse of the U_B-state. This collapsed state is called U_B' here without commenting on its possible structure and chain configuration. The chevron features and denaturant dependence of the amplitudes allow the possibility of the $U_B \rightleftharpoons B$ folding mechanism shown in Scheme 2, where I_n represents ensembles of folding and unfolding intermediates.

Scheme 2

$$U_B \rightleftharpoons U_B' \rightleftharpoons [\cdots I_n \cdots] \rightleftharpoons B$$

Folding Kinetics of B-, U_B-, and U-States at Neutral pH. To investigate the relevance of the molten globule state, the refolding kinetics of the alkali molten globule (B-state, pH 12.8, 2 M NaCl), the alkali-denatured state (U_B, pH 13), the GdnHCl-unfolded U_B-state (pH 13, 3.75 M GdnHCl), and the GdnHCl-unfolded protein at neutral pH (U, pH 7, 4.2 M GdnHCl) all at a final pH of 7 were studied as a function of GdnHCl. The inclusion of two sets of $U_B \rightarrow N$ experiments distinguished by the presence of GdnHCl in the initial U_B-state preparation was necessary, because the B-state is prepared at pH 12.8 with salt but the U-state is prepared at pH 7 by using GdnHCl. For all, the folding kinetics are essentially described by two exponentials, but a minor-amplitude third phase likely to arise from *cis*−*trans* proline isomerization was included to analyze the $U \rightarrow N$ refolding kinetics. Such a minor phase was occasionally observed in the refolding kinetics of other forms as well but will not be considered here. Since B and U_B are alkali forms and are refolded by a pH 13 → 7 jump as a function of GdnHCl at pH 7, the $B \rightleftharpoons N$ and $U_B \rightleftharpoons N$ equilibria do not exist under final refolding conditions. The process should rather be viewed as

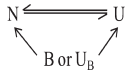

in the transition region strictly but can be approximated by $B \rightarrow N$ and $B \rightarrow U$ on either side.

The chevrons in Figure 5a show that refolding under moderate to strongly native-like conditions invariably occurs by a fast and a slow phase with macroscopic rate constants λ_1 and λ_2, respectively, λ_2 consistently rolls over, the folding kinetics in the transition region is monophasic, and hence two-state, the unfolding process in all cases occurs by a single observable phase, and the relaxation minimum in all instances occurs around 2.6 M GdnHCl which happens to be the C_m for the GdnHCl-induced equilibrium unfolding of ferricytochrome *c* at neutral pH (Figure 1d). Under strongly refolding conditions, the GdnHCl dependence of λ_1 is identical for $U \rightarrow N$ and $B \rightarrow N$ processes, but the value of λ_2 is consistently larger for the latter by ~4 times at all concentrations of GdnHCl despite apparently identical rate-denaturant gradients for the two, resulting in a vertically upward shift of the entire flat folding limb of the B−N chevron. The $U_B \rightarrow N$ and $U \rightarrow N$ folding limbs are very similar except for more conspicuous rollover of both λ_1 and λ_2 for the former. A slight downward translation of the U_B−N chevron is also noticeable (Figure 5a). The unfolding process for all reactions considered here (U, B, and U_B) is single exponential, and the unfolding limb of each chevron is distinguishable in terms of the rate-denaturant gradient or kinetic *m*-value ($m_u^‡$). The similarities of chevron features suggest that the millisecond folding mechanism is largely conserved even under very different initial conditions of pH, NaCl, and GdnHCl. The observed differences are due to variation in structure content and Gibbs free energies of U-, B-, and U_B-states.

For further analysis, the simplest two-state folding model of cytochrome *c* (*28*, *61*−*63*) may be invoked in a limited way in view of the inadequate knowledge of chevron behavior under extremes of denaturant concentration. The slow refolding phase (λ_2) of ferricyt *c* is known to arise from misfolding due to non-native histidine−heme ligation (*28*, *61*, *62*). When such misligations are blocked by employing appropriate solution conditions, λ_2 is completely suppressed, and λ_1 continues into the transition region displaying a two-state chevron. Even though the experimental conditions in the present study do not block the histidine−heme misligation which produces the slow phase (λ_2), the behavior of λ_1 can be examined separately. For all folding−unfolding reactions under scrutiny, Figure 5b shows the variation of λ_1 in

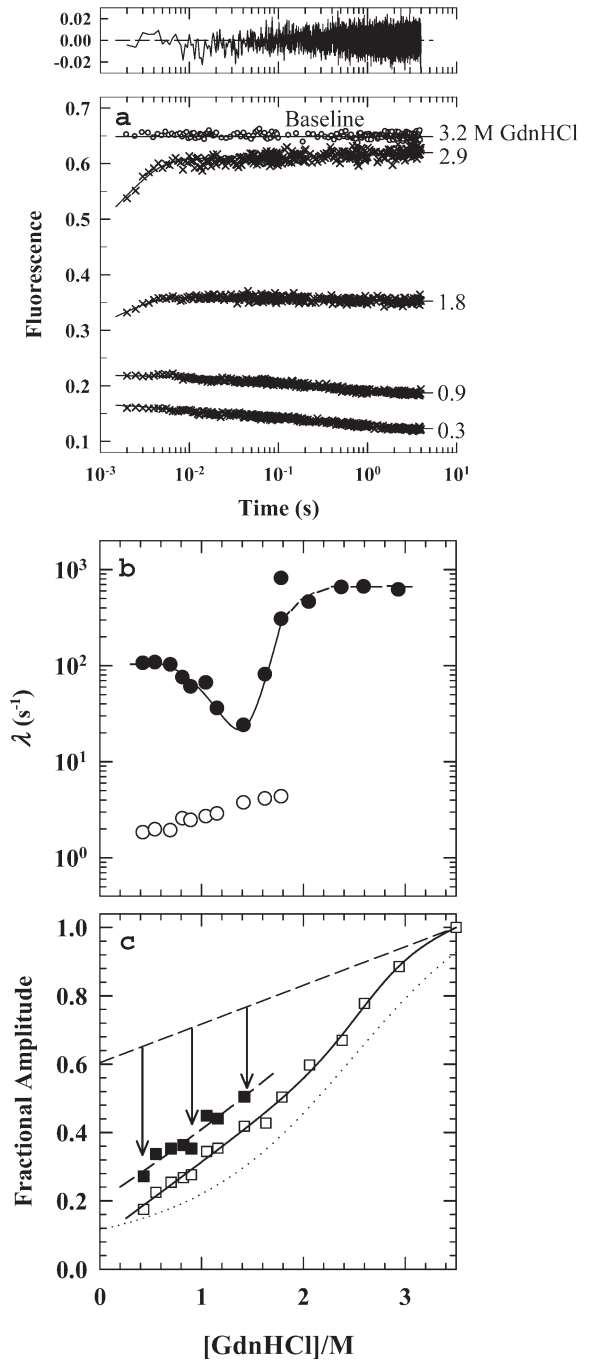

FIGURE 4: GdnHCl dependence of kinetics of the $U_B \rightleftharpoons B$ transition at pH 12.8. (a) Representative kinetic traces showing the burst change of fluorescence signal followed by two stopped-flow observable phases. (b) Denaturant dependence of the observed rate constants for the two phases, fast and slow (● and ○, respectively), shows a distinct chevron with flat limbs for the former; the slow phase vanishes at higher GdnHCl concentration. The solid line through the fast phase chevron has been drawn by inspection only. (c) The GdnHCl dependence of S_∞ (□) roughly matches the equilibrium $U_B \rightleftharpoons B$ transition reproduced from Figure 1c as dotted lines here (see Table 2). The GdnHCl dependence of the burst signal S_o (■) increases as strongly native-like conditions are approached (shown by arrows), suggesting an ultrafast collapse of the U_B-state.

the 0.8−4.2 M range of GdnHCl with iterated fits of data to the equation

$$\lambda = \lambda_{u,0} \exp\left(\frac{m_u^{\ddagger}[\text{GdnHCl}]}{RT}\right) + \lambda_{f,0} \exp\left(\frac{m_f^{\ddagger}[\text{GdnHCl}]}{RT}\right) \quad (3)$$

where, $\lambda_{u,0}$ and $\lambda_{f,0}$ are the apparent rate constants for unfolding and refolding in water and $m_u^{\ddagger}$ and $m_f^{\ddagger}$ are slopes of the unfolding and refolding limbs, respectively (Table 3). Values of $\lambda_{f,0}$ obtained from fits are in the 1000−1874 s^{-1} range, meaning near convergence of folding limbs under strongly native-like conditions despite substantially low $m_f^{\ddagger}$ value for the refolding of the B-state (Table 3). These results indicate similarities of millisecond refolding events for the alkali molten globule (B-state) and the unfolded state (U-state) regardless of the initial pH, solvent quality, and the extent of protein−solvent interactions. Significantly higher value of $\lambda_{u,0}$ and smaller $m_u^{\ddagger}$ for the B-state (Table 3) is due to its kinetic instability and the availability of lesser buried surface. The vertical displacements of the chevrons originate most likely from the rate-limiting steps dominated by diffusive motions of chain segments through the solution. Since the molten globule is already compact, large-scale diffusive migration of the main chain is allayed.

At very low concentrations of GdnHCl, λ_1 slightly rolls over for both B → N and U → N reactions almost identically (Figure 5c). Such a marginal rollover in the two-state folding of cytochrome *c* has been discussed in the past where the folding chevrons are quantified with a second-order polynomial version of eq 3. Under conditions where the histidine−heme misligation cannot be abrogated, λ_2 varies little at low concentrations of GdnHCl so as to produce a flat or marginally inverted folding limb (*64*), just the same way seen here for all reactions studied. This observation indicates that the ferric heme in the collapsed product of the B-state is liganded with non-native histidines (H26 and H33) irrespective of what served as the heme ligand initially at pH 12.8. Again, the larger value of λ_2 and hence the vertically upward translation of the flat B → N folding arm arise because the rate-limiting step for folding requires relatively small-scale diffusion of the protein segments.

All of these refolding reactions are associated with a submillisecond burst kinetic phase. The GdnHCl dependence of the burst amplitudes for U → N (Figure 6a) and U_B → N reactions (Figure 6b) are rather monotonous and featureless. The origin of this phase, whether from a sheer nonspecific chain contraction upon transfer of the protein chain from a good to a poor solvent or from a specific chain collapse, is uncertain (*65*−*70*). The burst data quality is almost always poor to allow an unambiguous quantitative analysis. It is also likely that the burst kinetics represent the occurrence of a sequence of polypeptide contracted states undergoing a higher order continuous transition in which case the amplitudes extracted may not show a cooperative transition expected for structured kinetic intermediate(s). However, as mentioned above, the B-state is an off-pathway species (Figures 2 and 3 and Scheme 1) that must unfold to be able to fold correctly. Accordingly, the corresponding burst species (U_B') should represent an unfolded-like state (Figure 6c). These observations are consistent with Scheme 3, where U′ is a nonspecifically contracted chain as described earlier (*71*), and I is a nonobligatory intermediate accumulated due to non-native histidine ligation to the heme (*28*). The collapsed species U_B' is likely to be more compact relative to U′, but the millisecond kinetic mechanisms are virtually identical for the two.

Scheme 3

$$U \longrightarrow U' \rightleftharpoons I \rightleftharpoons N$$

$$B \longrightarrow U_B' \rightleftharpoons I \rightleftharpoons N$$

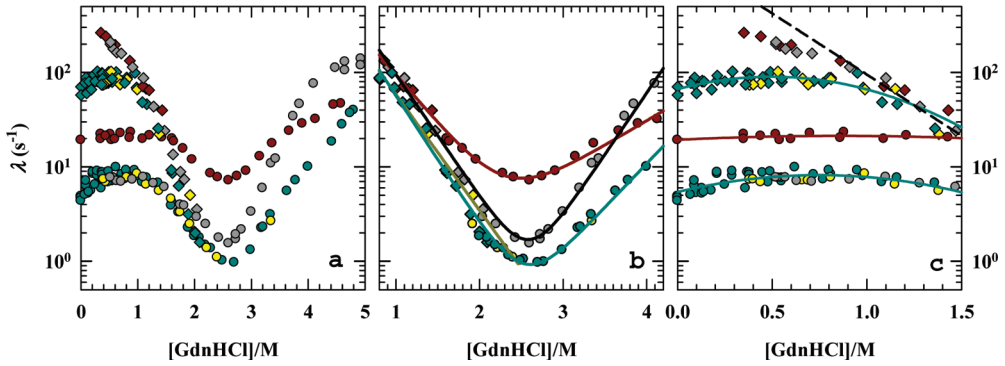

FIGURE 5: Chevron plots for the folding of the B-state (● and ◆ in red) carried out by pH 12.8, 2 M NaCl → pH 7, 0.25 M NaCl jump, the U_B-state (● and ◆ in green) and the U_B-state unfolded in 3.75 M GdnHCl (● and ◆ in yellow), both carried out by pH 13 → pH 7 jump, and the U-state unfolded in 4.2 M GdnHCl (● and ◆ in gray) by pH 7 → pH 7 jump. (a) Comparison of the four chevrons in the entire range of GdnHCl. (b) Fits of the chevrons in the two-state region (0.8−4.2 M GdnHCl) by the use of eq 3. (c) Details of λ-rollover under strongly native-like conditions where the fits require a second-degree polynomial dependence of the logarithm of λ.

Table 3: Kinetic Parameters for the Fast Phase of the Stopped-Flow Observable Folding Kinetics for U-, B-, and U_B-States at pH 7, 0.1 M Phosphate, 22 (±1) °C

reaction	$\lambda_{f,0}$ (s^{-1})	$m_f^{\ddagger}$ (kcal mol^{-1} M^{-1})	$\lambda_{u,0}$ (s^{-1})	$m_u^{\ddagger}$ (kcal mol^{-1} M^{-1})	C_m (M, GdnHCl)
U ⇌ N	1875 (±392)	−1.73 (±0.12)	0.000365	1.74 (±0.2)	~2.6
B ⇌ N	1043 (±103)	−1.40 (±0.06)	0.247 (±0.1)	0.7 (±0.09)	~2.6
U_B ⇌ N	1284 (±310)	−1.81 (±0.2)	0.0022	1.24 (±0.65)	~2.6

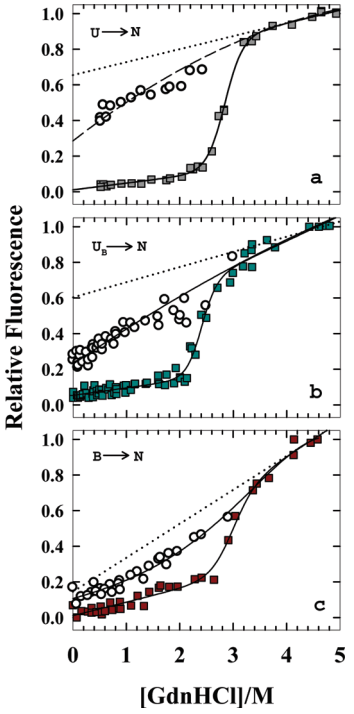

FIGURE 6: Amplitude analyses for various folding reactions indicated. In each, the colored solid symbols represent S_∞, the $t = \infty$ fluorescence obtained from exponential fits of the kinetic traces. The solid lines represent two-state fits that yield $\Delta G°$ values of 9.7, 9.7, and 8.0 kcal mol^{-1} for U → N, U_B → N, and B → N reactions, respectively. The corresponding values of m_g are 3.5, 4.0, and 2.7 kcal mol^{-1} M^{-1}. The GdnHCl dependences of burst signals (○) are fitted using empirical equations for data in (a) and (b). For (c) the dependence is fairly described by a two-state fit. In each panel, the dotted lines are approximate extrapolations of the unfolded baseline to the ordinate, and the area within this baseline and the burst signal represent the amplitude lost in the stopped-flow dead time.

To summarize the major results, ferricyt *c* alkali molten globule (B) is an off-pathway state that must expand to an unknown extent to achieve forward folding to the N-state. A number of kinetic intermediates appear to form in the putative molecular expansion process. This unfolded state (U_B') is expected to contain traces of secondary structure and is relatively more compact than the collapsed state (U′) formed during refolding of the GdnHCl-unfolded protein at neutral pH (U). The direct inaccessibility to the native state starting from the B-state suggests an uncertain role of the alkali molten globule in the folding of cytochrome *c*.

DISCUSSION

The B-State Fulfills All Criteria for a Classic Molten Globule. Results presented here and earlier rigorously define the cation-stabilized alkali equilibrium state of ferricytochrome *c* as an exemplary molten globule (*57*). The content of native-like α-helix and a fluid-like protein interior as indicated by dynamically averaged NMR lines, the absence of slow conformational exchange revealed by pure-exchange NMR spectroscopy, and sharp thermal unfolding transition and cold denaturation (*57*) are the principal attributes that qualify the B-state for a model molten globule (*14*, *16*, *34*, *72*). The hydrodynamic radius (22.1 ± 1.0 Å) is the only parameter by which the B-state could be seen relatively closer to U_B (Table 1). Notwithstanding this slight drift of R_H toward the upper bound, the molecular dimension and density of the B-state remain within the canonical range (*73*−*75*). Hence, the B-state considered here is highly ordered and could serve for examining the role of the molten globule intermediate in cytochrome *c* folding.

Under Alkaline Conditions the B-State Cannot Access the Native State Directly. The hallmark of the B-state refolding under alkaline condition is a burst molecular expansion to a kinetic species B′ that expands further via one or more millisecond intermediates to give rise to the U_B-state which proceeds to fold to N_B presumably involving intermediates (Figures 2 and 3b and Scheme 1). The implication here that the B-state is a nonproductive off-pathway species is antithesis to the tenet that molten globules are obligatory on-pathway folding intermediates

(*14*, *76*−*78*). To analyze whether or not this result violates the belief of the on-pathway role of molten globules, a detailed structural and dynamical picture of the B-state is essential. As previously discussed, a variety of information available thus far indicates that the B-state distinctively fulfills all criteria of a molten globule (*57*). Then a conservative note is that molten globules do not invariably have a productive role in protein folding, just as the assertion of one of the earlier papers that they might as well represent off-pathway species (*79*). However, numerous evidence in favor of molten globules' productive role warrants a scrutiny for possible conformational events due to proton linkage and electrostatic interactions which may force the B-state chain to expand when folding is initiated. In the case of cytochrome *c* the ionization of lysyl side chains (ε-$NH_3^+ \rightarrow \varepsilon$-$NH_2 + H^+$) at alkaline pH could be a suspect, even though the spectroscopic and hydrodynamic probes used earlier (*57*) and now have not reported so. In trans-pH folding experiments, folding is fundamentally driven by, although in a complex manner, proton binding and electrostatic interactions. Even if the protocol employed here, pH 12.9, 2 M NaCl (initial) → pH 11.5, 1.5 M NaCl, variable GdnHCl concentration (final), avoids a drastic change in H^+ concentration and ionic strength between the initial and final conditions, the ionization status of lysine and tyrosine side chains may change considerably. The calculated pK_a values for the ε-NH_3^+ groups of the 19 lysine residues of native cytochrome *c* at pH 7 lie in the 9.5−13.4 range, and holding the protein under solution conditions as employed here will shift the pK_a of individual residues and hence influence the ligation of ε-NH_3^+ groups with the ferric heme in a pH- and ionic strength-dependent manner. In a bid to reorganize the chain configuration caused by reshuffling of non-native heme ligands during refolding, the B-state may expand to some extent. Thus, the results for B-state refolding under alkaline conditions seem inconclusive to assign a role for the molten globule. This matter is taken up further in the companion paper (*43*) where ligand-related complications irrespective of the pH of the folding medium are suppressed by using ferrocytochrome *c*.

The B-State First Unfolds When Driven To Fold at Neutral pH. Because of similar chain topology between the equilibrium molten globule and the native state, the MG → N transition is expected to be much faster than the U → N transition. The expectation is much higher for the B-state of ferricyt *c* which possesses an unusually ordered water-shielded hydrophobic core as earlier inferred from its cooperative thermal unfolding accompanied by a sizable heat capacity change (*57*). Contrary to the expectation, when placed under native conditions at pH 7, the B-state refolds as slowly as the alkali-unfolded or GdnHCl-unfolded state does, meaning the operation of the same rate-limiting barrier (Figure 6). In fact, the B → N and U → N reactions proceed by similar kinetic mechanisms; albeit the structural organizations of the corresponding species in the two reaction pathways are distinct. Thus when allowed to fold, the B-state expands and collapses to a compact state that has to surmount the main energy barrier for folding. The unfolded state and the collapsed product involved in the B → N reaction are different from the corresponding species for the U → N process, because the denaturant dependence of the burst signal is different for the two and the chevron for the former is vertically shifted upward with shallower limbs.

The B-State of Ferricyt c Is Not a Good Model for Kinetic Molten Globule. The inability of the B-state to fold directly to the native state counters the widely accepted belief that molten globules are equilibrium models of kinetic folding intermediates (*3*, *35*, *37*−*40*). The alkali molten globule of cytochrome *c* does not represent any kinetic intermediate and hence is irrelevant for the kinetic folding of the protein. This is the third case reported for the lack of such a correlation since the finding of substantial structural differences between the equilibrium A-state and neutral pH kinetic molten globule intermediates of apoleghemoglobin (*41*) and α-lactalbumin (*42*). In the case of apoleghemoglobin where the refolding experiment was done by stopped-flow pH jump from acidic to neutral pH values, the authors appear to attribute the lack of correlation of equilibrium and kinetic molten globule to the influence of pH on the energy landscape (*41*). The trans-pH energy landscape differences may not however explain the present results fully, because the B-state (prepared at pH 12.9) cannot access the native state at both pH 11.5 and pH 7 unless it unfolds first. A direct demonstration of the initial chain expansion is provided by the set of refolding experiments involving a pH 12.9 → pH 11.5 jump (see Figures 2 and 3), although it is not implied that the initial unfolding of the B-state produces the same species irrespective of the final refolding pH. Even if the effects of proton binding and electrostatic interactions are minimized, as in the pH 12.9 → pH 11.5 refolding experiment, the undesirable heme−lysine misligation may force the B-state to expand and unfold. The study in the companion paper (*43*) was initiated to further minimize any residual trans-pH effect and to avoid the possible influence of heme misligation during refolding.

REFERENCES

1. Fink, A. L. (2005) Natively unfolded proteins. *Curr. Opin. Struct. Biol. 15*, 35–41.
2. Uversky, V. N. (2002) Natively unfolded proteins: a point where biology waits for physics. *Protein Sci. 11*, 739–756.
3. Dyson, H. J., and Wright, P. E. (2002) Coupling of folding and binding for unstructured proteins. *Curr. Opin. Struct. Biol. 12*, 54–60.
4. Tompa, P. (2002) Intrinsically unstructured proteins. *Trends Biochem. Sci. 27*, 527–533.
5. Uversky, V. N. (2002) What does it mean to be natively unfolded? *Eur. J. Biochem. 269*, 2–12.
6. Bychkova, V. E., Pain, R. H., and Ptitsyn, O. B. (1988) The "molten globule" state is involved in the translocation of proteins across membranes. *FEBS Lett. 238*, 231–234.
7. Nakayama, K. I., Hatakeyama, S., and Nakayama, K. (2001) Regulation of the cell cycle at the G1-S transition by proteolysis of cyclin E and P27Kip1. *Biochem. Biophys. Res. Commun. 282*, 853–860.
8. Dunker, A. K., Cortese, M. S., Romero, P., Iakoucheva, L. M., and Uversky, V. N. (2005) Flexible nets. The roles of intrinsic disorder in protein interaction networks. *FEBS J. 272*, 5129–5148.
9. Kokai, E., Tantos, A., Vissi, E., Szoor, B., Tompa, P., Gausz, J., Alphey, L., Friedeich, P., and Dombradi, V. (2006) CG15031/PPYR1 is an intrinsically unstructured protein that interacts with protein phosphatase Y. *Arch. Biochem. Biophys. 451*, 59–67.
10. Radivojac, P., Vucetic, S., O'Connor, T. R., Uversky, V. N., Obradovic, Z., and Dunker, A. K. (2006) Calmodulin signaling: analysis and prediction of a disorder-dependent molecular recognition. *Proteins 63*, 398–410.
11. Tompa, P., Banki, P., Bokor, M., Kamasa, P., Kovacs, D., Lasanda, G., and Tompa, K. (2006) Protein-water and protein-buffer interactions in the aqueous solution of an intrinsically unstructured plant dehydrin: NMR intensity and DSC aspects. *Biophys. J. 91*, 2243–2249.
12. Baker, B. Y., Yaworsky, D. C., and Miller, W. L. (2005) A pH-dependent molten globule transition is required for activity of the steroidogenic acute regulatory protein StaR. *J. Biol. Chem. 280*, 41753–41760.
13. Tompa, P. (2003) Intrinsically unstructured proteins evolve by repeat expansion. *BioEssays 25*, 847–855.
14. Ptitsyn, O. B. (1995) Molten globule and protein folding. *Adv. Protein Chem. 47*, 83–229.
15. Kuwajima, K., and Arai, M. (2000) The molten globule state: the physical and biological significance, in Mechanism of Protein Folding

(Pain, R. H., Ed.) 2nd ed., pp 138−174, Oxford University Press, New York.
16. Arai, M., and Kuwajima, K. (2000) Role of the molten globule state in protein folding. *Adv. Protein Chem. 53*, 209–271.
17. Pandey, V. S., and Rokhsar, D. S. (1998) Is the molten globule a third phase of proteins? *Proc. Natl. Acad. Sci. U.S.A. 95*, 1490–1494.
18. Baldwin, R. L., and Rose, G. D. (1999) Is protein folding hierarchic? I. Local structure and peptide folding. *Trends Biochem. Sci. 24*, 26–33.
19. Yeh, S. R., and Rousseau, D. L. (2000) Hierarchical folding of cytochrome *c*. *Nat. Struct. Biol. 7*, 443–445.
20. Akiyama, S., Takahashi, S., Ishimori, K., and Morishima, I. (2000) Stepwise formation of α-helices during cytochrome *c* folding. *Nat. Struct. Biol. 7*, 514–520.
21. Jennings, P. A., and Wright, P. E. (1993) Formation of a molten globule intermediate early in the kinetic folding pathway of apomyoglobin. *Science 262*, 892–896.
22. Raschke, T. M., and Marqusee, S. (1997) The kinetic folding intermediate of ribonuclease H resembles the acid molten globule and partially unfolded molecules detected under native conditions. *Nat. Struct. Biol. 4*, 298–304.
23. Nishimura, C., Riley, R., Eastman, P., and Fink, A. L. (2000) Fluorescence energy transfer indicates similar transient and equilibrium intermediates in staphylococcal nuclease folding. *J. Mol. Biol. 299*, 1133–1146.
24. Engelhard, M., and Evans, P. A. (1995) Kinetics of interaction of partially folded proteins with a hydrophobic dye: evidence that molten globule character is maximal in early folding intermediates. *Protein Sci. 4*, 1553–1562.
25. Wolynes, P. G., Onuchic, J. N., and Thirumalai, D. (1995) Navigating the folding routes. *Science 267*, 1619–1620.
26. Colón, W., and Roder, H. (1996) Kinetic intermediates in the formation of the cytochrome *c* molten globule. *Nat. Struct. Biol. 3*, 1019–1025.
27. Mok, K. H., Nagashima, T., Day, I. J., Hore, P. J., and Dobson, C. M. (2005) Multiple subsets of side-chain packing in partially folded states of α-lactalbumins. *Proc. Natl. Acad. Sci. U.S.A. 102*, 8899–8904.
28. Sosnick, T. R., Mayne, L., Hiller, R., and Englander, S. W. (1994) The barriers in protein folding. *Nat. Struct. Biol. 1*, 149–156.
29. Nishimura, C., Dyson, H. J., and Wright, P. E. (2002) The apomyoglobin folding pathway revisited: structural heterogeneity in the kinetic burst phase intermediate. *J. Mol. Biol. 322*, 483–489.
30. Jennings, P. A., and Wright, P. E. (1993) Formation of a molten globule intermediate early in the kinetic folding pathway of apomyoglobin. *Science 262*, 892–896.
31. Ikeguchi, K., Kuwajima, K., Mitani, M., and Sugai, S. (1986) Evidence for identity between the equilibrium unfolding intermediate and a transient folding intermediate: a comparative study of the folding reactions of α-lactalbumin and lysozyme. *Biochemistry 25*, 6965–6972.
32. Raschke, T. M., and Marqusee, S. (1997) The kinetic folding intermediate of ribonuclease H resembles the acid molten globule and partially unfolded molecules detected under native conditions. *Nat. Struct. Biol. 4*, 298–304.
33. Fujiwara, K., Arai, M., Shimizu, A., Ikeguchi, M., Kuwajima, K., and Sugai, S. (1999) Folding-unfolding equilibrium and kinetics of equine β-lactoglobulin: equivalence between the equilibrium molten globule state and a burst phase folding intermediate. *Biochemistry 38*, 4455–4463.
34. Kuwajima, K. (1989) The molten globule state as a clue for understanding the folding and coopertivity of globular-protein structure. *Proteins 6*, 87–103.
35. Matthews, C. R. (1993) Pathways of protein folding. *Annu. Rev. Biochem. 62*, 653–683.
36. Evans, P. A., and Radford, S. E. (1994) Probing the structure of folding intermediates. *Curr. Opin. Struct. Biol. 4*, 100–106.
37. Ptitsyn, O. B. (1994) Kinetic and equilibrium intermediates in protein folding. *Protein Eng. 7*, 593–596.
38. Hughson, F. M., Wright, P. E., and Baldwin, R. L. (1990) Structural characterization of a partly folded apomyoglobin intermediate. *Science 249*, 1544–1548.
39. Kuwajima, K. (1996) The molten globule state of α-lactalbumin. *FASEB J. 10*, 102–109.
40. Privalov, P. L. (1996) Intermediate states in protein folding. *J. Mol. Biol. 258*, 707–725.
41. Nishimura, C., Dyson, H. J., and Wright, P. E. (2008) The kinetic and equilibrium molten globule intermediates of apomyoglobin differ in structure. *J. Mol. Biol. 378*, 715–725.
42. Rösner, H. I., and Redfield, C. (2009) The human α-lactalbumin molten globule: comparison of structural preferences at pH 2 and pH 7. *J. Mol. Biol. 394*, 351–362.
43. Bhuyan, A. K. (2010) The off-pathway status of the alkali molten globule is unrelated to heme misligation and trans-pH effects: experiments with ferrocytochrome *c*, *Biochemistry* (DOI 10.1021/bi100881n).
44. Ohgushi, M., and Wada, A. (1983) "Molten globule state": a compact form of globular proteins with mobile side-chains. *FEBS Lett. 164*, 21–24.
45. Robinson, J. B. J., Strottmann, J. M., and Stellwagen, E. A. (1983) A globular high spin form of ferricytochrome *c*. *J. Biol. Chem. 258*, 6772–6776.
46. Potekhin, S., and Pfeil, W. (1989) Microcalorimetric studies of conformational transitions of ferricytochrome *c* in acidic solution. *Biophys. Chem. 34*, 55–62.
47. Goto, Y., Calciano, L. J., and Fink, A. L. (1990) Acid-induced folding of proteins. *Proc. Natl. Acad. Sci. U.S.A. 87*, 573–577.
48. Jeng, M.-F., Englander, S. W., Elöve, G. A., Wand, A. J., and Roder, H. (1990) Structural description of acid denatured cytochrome *c* by hydrogen exchange and 2D NMR. *Biochemistry 29*, 10433–10437.
49. Jeng, M.-F., and Englander, S. W. (1991) Stable submolecular folding units in a non-compact form of cytochrome *c*. *J. Mol. Biol. 221*, 1045–1061.
50. Kuroda, Y., Kidokoro, S., and Wada, A. (1992) Thermodynamic characterization of cytochrome *c* at low pH. *J. Mol. Biol. 223*, 1139–1153.
51. Kataoka, M., Hagihara, Y., Mihara, K., and Goto, Y. (1993) Molten globule of cytochrome *c* studied by small angle X-ray scattering. *J. Mol. Biol. 229*, 591–596.
52. Hagihara, Y., Tan, Y., and Goto, Y. (1994) Comparison of the conformational stability of the molten globule and native states of horse cytochrome *c*: effects of acetylation, heat, urea, and guanidine-hydrochloride. *J. Mol. Biol. 237*, 336–348.
53. Kuroda, Y., Endo, S., Nagayama, K., and Wada, A. (1995) Stability of α-helices in a molten globule state of cytochrome *c* by hydrogen-deuterium exchange and two-dimensional NMR spectropscopy. *J. Mol. Biol. 247*, 682–688.
54. Chalikian, T. V., Gindikin, V. S., and Breslauer, K. J. (1995) Volumetric characterizations of the native, molten globule, and unfolded states of cytochrome *c* at acidic pH. *J. Mol. Biol. 250*, 291–306.
55. Jordan, T., Eads, J. C., and Spiro, T. G. (1995) Secondary and tertiary structure of the A-state of cytochrome *c* from resonance Raman spectroscopy. *Protein Sci. 4*, 716–728.
56. Rao, D. K., Kumar, R., Yadaiah, M., and Bhuyan, A. K. (2006) The alkali molten globule state of ferrocytochrome *c*: extraordinary stability, persistent structure, and constrained overall dynamics. *Biochemistry 45*, 3412–3420.
57. Kumar, R., Prabhu, N. P., Rao, D. K., and Bhuyan, A. K. (2006) The alkali molten globule state of horse ferricytochrome *c*: observation of cold denaturation. *J. Mol. Biol. 364*, 483–495.
58. Goto, Y., and Fink, A. L. (1989) Conformational states of β-lactamase: molten globule states at acidic and alkaline pH with high salt. *Biochemistry 28*, 945–952.
59. Rami, B. R., and Udgaonkar, J. B. (2002) Mechanism of formation of a productive molten globule form of barstar. *Biochemistry 41*, 1710–1716.
60. Altieri, A. S., Hinton, D. P., and Byrd, R. A. (1995) Association of biomolecular systems via pulsed field gradient NMR self-diffusion measurements. *J. Am. Chem. Soc. 117*, 7566–7567.
61. Sosnick, T. R., Mayne, L., and Englander, S. W. (1996) Molecular collapse: the rate-limiting step in two state cytochrome *c* folding. *Proteins: Struct., Funct., Genet. 24*, 413–426.
62. Bhuyan, A. K., and Udgaonkar, J. B. (2001) Folding of horse cytochrome *c* in the reduced state. *J. Mol. Biol. 312*, 1135–1160.
63. Prabhu, N. P., Kumar, R., and Bhuyan, A. K. (2004) Folding barrier in horse cytochrome *c*: support for a classical folding pathway. *J. Mol. Biol. 337*, 195–208.
64. Bai, Y. (1999) Kinetic evidence for an on-pathway intermediate in the folding of cytochrome *c*. *Proc. Natl. Acad. Sci. U.S.A. 96*, 477–480.
65. Roder, H., and Colon, W. (1997) Kinetic role of early intermediates in protein folding. *Curr. Opin. Struct. Biol. 7*, 15–28.
66. Sosnick, T. R., Shtilerman, M. D., Mayne, L., and Englander, S. W. (1997) Ultrafast signals in protein folding and the polypeptide contracted state. *Proc. Natl. Acad. Sci. U.S.A. 94*, 8545–8550.
67. Shastry, M. C. R., and Roder, H. (1998) Evidence for barrier-limited protein folding kinetics on the microsecond time scale. *Nat. Struct. Biol. 5*, 385–392.
68. Qi, P. Q., Sosnick, T. R., and Englander, S. W. (1998) The burst phase in ribonuclease A folding: solvent dependence of the unfolded state. *Nat. Struct. Biol. 5*, 882–884.
69. Bhuyan, A. K., and Udgaonkar, J. B. (1999) Relevance of burst phase changes in optical signals of polypeptides during protein folding, in Perspectives in Structural Biology (Vijayan, M., et al., Eds.) pp 293−303, University Press, Hyderabad, India.

70. Kumar, R., and Bhuyan, A. K. (2005) Two-state folding of horse ferrocytochrome *c*: analyses of linear free energy relationship, chevron curvature, and stopped-flow burst relaxation kinetics. *Biochemistry 44*, 3024–3033.
71. Bhuyan, A. K., Rao, D. K., and Prabhu, N. P. (2005) Protein folding in classical perspective: folding of horse cytochrome *c*. *Biochemistry 44*, 3034–3040.
72. Christensen, H, and Pain, R. H. (1991) Molten globule intermediates and protein folding. *Eur. Biophys. J. 19*, 221–229.
73. Kataoka, M., Kuwajima, K., Tokunaga, F., and Goto, Y. (1997) Structural characterization of the molten globule of alpha-lactalbumin by solution X-ray scattering. *Protein Sci. 6*, 422–430.
74. Uversky, V. N. (2003) Protein folding revisited. A polypeptide chain at the folding-misfolding-nonfolding cross-roads: which way to go. *CMLS, Cell. Mol. Life Sci. 60*, 1852–1871.
75. Kohn, J. E., Gillespie, B., and Plaxco, K. W. (2009) Non-sequence-specific interactions can account for the compaction of proteins unfolded under native conditions. *J. Mol. Biol. 394*, 343–350.
76. Arai, M., and Kuwajima, K. (1996) Rapid formation of a molten globule intermediate in refolding of α-lactalbumin. *Folding Des. 1*, 275–287.
77. Raschke, T. M., Kho, J., and Marqusee, S. (1999) Confirmation of the hierarchical folding of RNase H: a protein engineering study. *Nat. Struct. Biol. 6*, 825–831.
78. Nakamura, T., Makabe, K., Tomoyori, K., Maki, K., Mukaiyama, A., and Kuwajima, K. (2010) Different folding pathways taken by highly homologous proteins, goat α-lactalbumin and canine milk lysozyme. *J. Mol. Biol. 396*, 1361–1378.
79. Creighton, T. E. (1997) How important is the molten globule for correct protein folding. *Trends Biochem. Sci. 22*, 6–10.